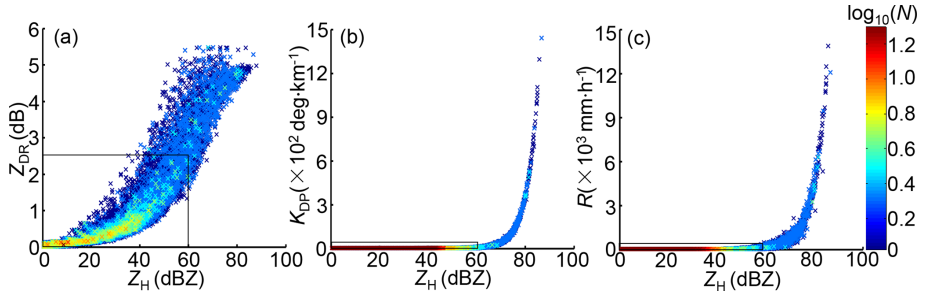

Figure 7. The scattergrams of DSD-derived polarimetric radar variables without QC processing: **(a)** Z_{DR} vs. Z_H, **(b)** K_{DP} vs. Z_H, **(c)** R vs. Z_H. The rectangles in **(a–c)** indicate the ranges of DSD-derived variables after final QC processing.

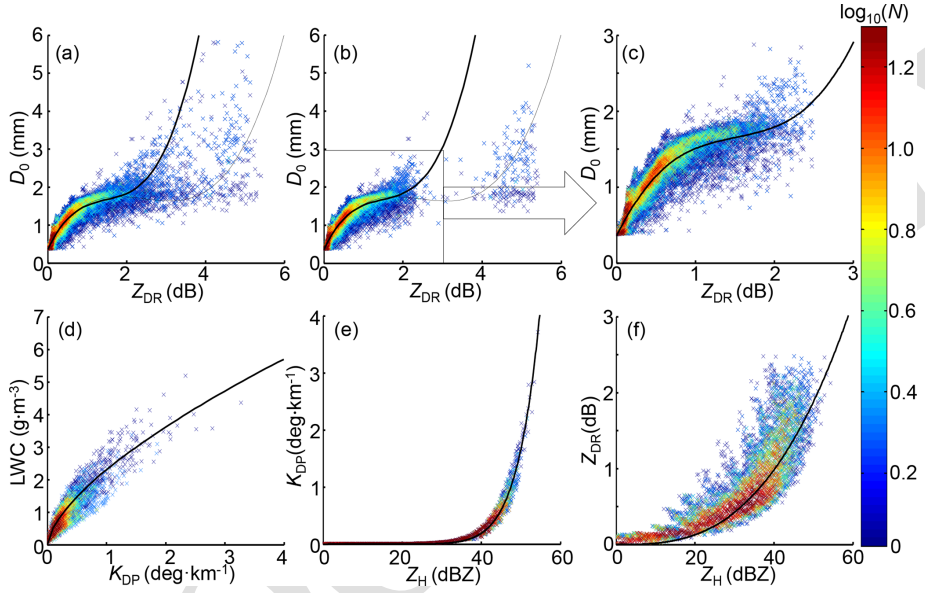

Figure 8. Scattergrams between polarimetric radar variables: **(a)** D_0 vs. Z_{DR} after eliminating wind contaminations. Panel **(b)** is based on **(a)** but after removing the hail and graupel contaminations further. Panel **(c)** is based on **(b)** but after further eliminating the residual graupel contaminations with $Z_{DR} > 2.5$ dB. Panels **(d)**, **(e)**, and **(f)** are LWC vs. K_{DP}, K_{DP} vs. Z_H, and Z_{DR} vs. Z_H based on the same dataset as **(c)**. The thick black lines in **(a)**–**(c)** stand for Eq. (5); the thin black lines in **(a)** and **(b)** indicate the overfitted results, and the black curves in **(d)**-**(f)** stand for Eqs. (6), (7), and (2a), respectively.

lationship in Eq. (2a) (see Fig. 8f):

$$D_0 = 0.2987 \times Z_{DR}^3 - 1.3229 \times Z_{DR}^2 + 2.1931 \times Z_{DR} + 0.3543, \quad (6)$$

$$\mathrm{LWC} = 2.0949 \times K_{DP}^{0.6889}, \quad (7)$$

$$K_{DP} = 1.5473 \times 10^{-13} \times Z_H^{8.8365}. \quad (8)$$

TS4 Combining these relationships and another relationship between the normalized concentration of raindrops (N_w, CF4), LWC, and the mean volume diameter of the drop size distribution (D_m, in mm) in Eqs. (9) and (10),

$$N_w = \frac{4^4}{\pi \rho_w} \frac{\mathrm{LWC}}{D_m^4}, \quad (9)$$

$$D_m = \frac{4+\mu}{3.67+\mu} D_0, \quad (10)$$

where ρ_w is the water density (1 g cm^{-3}). High-resolution DSD parameter fields can be derived from WZ-SPOL radar measurements.

3.1.2 The self-consistency between radar measurements

The self-consistency can demonstrate the credibility of polarimetric radar measurements through scattergrams (Fig. 9). The scattergrams in Fig. 9b and d are obtained from all Z_H^C, Z_{DR}^C, and K_{DP} measurements described in Fig. 11. The ZHPI approach (Bringi et al., 2001) with more constraints described in Gou et al. (2019a) effectively mitigates the attenuation effects on Z_H and Z_{DR} of the WZ-SPOL radar. The spatial fields of Z_H^M and Z_{DR}^M are not presented (they will not be used for the subsequent analysis), but it is noticeable that